

Tracking Maneuver Target Using 3D Position Forecast Model with Estimated Speed by Least Squares Method

Agner Júnior J¹, Schulze B², Mury A R³, Ferro M⁴, dos Santos M⁵

Abstract Tracking targets is a complex process, which requires association algorithms capable of handling the use of linear and nonlinear filtering techniques. It is known that the two-dimensional models of air traffic control systems are insufficient for the treatment of three-dimensional maneuvers of military targets, due to considerable variations in altitude. The work was based on flight dynamics models, which describe the evolution of the state of a target, treated as a punctual object in three-dimensional trajectories, addressing the problem of its movement uncertainty. The adopted model has application in civil and military navigation and surveillance systems, allowing the tracking of targets in real time. The Kalman Filter (KF) and the Extended Kalman Filter (EKF) were adopted as state estimators with integration through the filter of hybrid systems Interacting Multiple Models (IMM). The innovation of the work is in obtaining the scalar velocities of each Cartesian axis to be part of the vector of \mathbf{z}_k , observations, through the Method of Least Squares, resulting in greater precision than in previous works. Numerical examples illustrate the applicability and performance of the proposed method.)

Keywords: 3D Object Position, Kalman Filter, Interacting Multiple-Model.

1 Introduction

This paper develops a new method of obtaining the vector velocity components of measurements of a given sensor, from the information of an object in space applying the Method of Least Squares (MLS). This new method, applied to the work model presented in Agner Júnior et al. (2020), demonstrates a significant improvement in the accuracy of the estimated position of the measured object.

The problem of predicting the position of maneuvering objects is not a trivial task, as it requires several studies and varied analyzes, not only of a conceptual nature, but also of a practical order. Several models have been developed to improve existing solutions, such as those described in Frencl and Val (2012a), Yuan, Lian and Han (2014), Liu et al. (2018), among others.

The prediction of object positions is based on the estimation theory, which has the purpose of developing estimators, also known as filters, which have the possibility of being applied to engineering problems, such as orbit and altitude estimation, power, fault detection, surveillance and determination of

¹Jair Agner Júnior (e-mail: jairagnerjunior@gmail.com)

Divisão de Pesquisa Operacional. Centro de Análises de Sistemas Navais. Praça Barão de Ladário s/no - Ilha das Cobras - Rua da Ponte, Ed. 23 do AMRJ – Centro, Rio de Janeiro – RJ, Brasil

²Bruno Schulze (e-mail: schulze@lncc.br)

Laboratório Nacional de Computação Científica (LNCC). Av. Getúlio Vargas, 333 – Quitandinha, Petrópolis – RJ, Brasil

³Antônio Roberto Mury (e-mail: a.roberto.m@gmail.com)

Laboratório Nacional de Computação Científica (LNCC). Av. Getúlio Vargas, 333 – Quitandinha, Petrópolis – RJ, Brasil

⁴Mariza Ferro (e-mail: mariza@lncc.br)

Laboratório Nacional de Computação Científica (LNCC). Av. Getúlio Vargas, 333 – Quitandinha, Petrópolis – RJ, Brasil

⁵Marcos dos Santos (e-mail: marcosdossantos_doutorado_uff@yahoo.com.br)

Divisão de Pesquisa Operacional. Centro de Análises de Sistemas Navais. Praça Barão de Ladário s/no - Ilha das Cobras - Rua da Ponte, Ed. 23 do AMRJ – Centro, Rio de Janeiro – RJ, Brasil

the future positioning of targets by radar or sonar, integrated navigation, among others (Bar-Shalom, Li and Kirubarajan, 2001). In this context, we try to estimate the state variables of a linear or nonlinear stochastic system through filtering. In this way, models are developed to be used in the filtering, which seek to represent these state variables in an approximate way, which allows to obtain a solution for estimating the future positions of objects in motion.

Among the great variety of existing dynamic models, two were chosen for the elaboration of this work, which deal with objects in displacement: the model with Constant Velocity (CV), implemented with the Kalman Filter (KF) to deal with linear filtering and the Constant Turn (CT), implemented with the Extended Kalman Filter (EKF) to cover nonlinear filtration. The CV and CT models represent particular cases of the kinematic model of Planar Curvilinear Motion with two-dimensional movement dynamics (Korbicz et al., 2004).

To use more than one model in a state estimation problem, one must use a technique that allows the use of models in parallel. The approach adopted to work with multiple models in parallel was the Interacting Multiple-Model (IMM) algorithm, proposed in Bar-Shalom et al. (1988). The IMM estimates the state of a dynamic system and its respective covariance matrix through the weighted sum of the estimates of N KF models executed in parallel. It is an estimation tool that in each iteration the weighting factors are calculated for the combination of the estimates of each of the filter models. The implementation of IMM was necessary, because an object moving in space can develop different behavior patterns over time, and the use of only one filter becomes inefficient to adapt to these behavioral variations. Thus, the IMM was used to work simultaneously with the KF (using the CV model) and with the EKF (using the CT model).

2 Mathematical Models

Many of the object positioning prediction techniques are described using models, which are based on the behavioral aspects and observations of the target. Behavior is usually represented in the form of a dynamic or motion model, also called a state model, describing the evolution of several physical quantities, such as position and speed. The aspect that deals with the observations of the object is represented through observation models (Frencl, 2010). Thus, to adequately treat the position prediction problem, mathematical models are described, taking into account the relevant equations, variables and parameters.

Equations (1) and (2) define KF and EKF, which are described in detail with applications in Bar-Shalom, Li and Kirubarajan (2001) and Welch and Bishop (2001). However, in this work the Kalman Filter solves the general problem of seeking to estimate the state $\mathbf{x} \in \mathbf{R}^8$, of a process controlled in discrete time that is governed by the linear stochastic difference equation (1), with a measurement $\mathbf{z}_k \in \mathbf{R}^5$, (2) described by:

$$\mathbf{x}_{k+1} = \mathbf{F}_k \mathbf{x}_k + \mathbf{G}_k \mathbf{u}_k + \mathbf{B}_k \mathbf{w}_k, \quad (1)$$

$$\mathbf{z}_{k+1} = \mathbf{H}_{k+1} \mathbf{x}_{k+1} + \mathbf{v}_{k+1} \quad (2)$$

The state estimation performed by Equation (1) obeys the laws that govern the movement of the object that is in displacement. These laws, as well as the approach adopted for calculating the measurements made by Equation (2), will be described later. The random variables \mathbf{w}_k e \mathbf{v}_{k+1} represent process noise and measurement noise, respectively. They are considered normal (Gaussian) distribution, independent, identically distributed, with zero mean and covariance \mathbf{Q} and \mathbf{R} , respectively. Thus, $p(\mathbf{w}) \sim N(0, \mathbf{Q})$ e $p(\mathbf{v}) \sim N(0, \mathbf{R})$. The state transition matrix $\mathbf{F}_{8 \times 8}$, in Equation (1), refers to the state of the sample in the previous time interval k , to the current state in time $k + 1$.

The matrix $\mathbf{G}_{8 \times 5}$ refers to the optional control input $\mathbf{u}_k \in \mathbf{R}^5$, for state \mathbf{x}_{k+1} . In this approach, the control input \mathbf{u}_k can be assigned as the noise of the sensor position that makes the object position measurement.

Thus, the movement of the sensor has an influence on the position of the object. The $\mathbf{G}_{8 \times 5}$ matrix controls the effects of \mathbf{u}_k , and as this work is considered a static observer, the term $\mathbf{G}_k \mathbf{u}_k$ is not

incorporated in the process equation. The $\mathbf{B}_{8 \times 5}$ matrix controls the effects of \mathbf{w}_k . The matrix $\mathbf{H}_{5 \times 8}$, in the Measurement Equation (2), relates the state to the measure \mathbf{z}_{k+1} .

To develop this work, it was necessary to adopt a model of observations for the object to be studied. Thus, the measurements of a simulated radar system and the object as an aircraft (target) were used as a reference. These measures were represented in the form of the vector $\mathbf{z}_k = [\mathbf{r}_k \ \theta_k \ \phi_k]^T$, where \mathbf{r}_k is the distance in meters from the object to the observer, θ_k is the azimuth angle measured in degrees from the geographical north to the center of the object and ϕ_k is the elevation angle in degrees measured from a null horizontal reference (horizontal plane, in the case of sea level) to the center of the object. It is known that these measurements are disturbed by noise (or errors), in distance (\mathbf{v}_k^r), in the azimuth angle (\mathbf{v}_k^θ) and in the elevation angle (\mathbf{v}_k^ϕ), the which are assumed to be independent and stationary with Gaussian distribution of zero mean and constant variances σ_r , σ_θ e σ_ϕ , respectively.

The study object was treated punctually, described in three dimensions, with the position vector represented by $\mathbf{r}(t) = [\mathbf{x}(t) \ \mathbf{y}(t) \ \mathbf{h}(t)]^T$, in Cartesian coordinates. For the dynamic or motion model, were used as state variables: x , y (horizontal coordinates), h (altitude), χ (bow or heading angle - horizontal), γ (trajectory angle - vertical), \mathbf{v} (velocity vector) and \mathbf{a} (acceleration vector).

Equations (3), (4) and (5) are obtained from the derivative of the $\mathbf{r}(t)$ components describe the object's velocity as a function of Cartesian coordinates relating the instantaneous tangential velocity $\mathbf{v}(t)$, χ and γ .

$$\mathbf{v}_x(t) = \mathbf{v}(t) \cdot \cos(\chi(t)) \cdot \cos(\gamma(t)) \quad (3)$$

$$\mathbf{v}_y(t) = \mathbf{v}(t) \cdot \sin(\chi(t)) \cdot \cos(\gamma(t)) \quad (4)$$

$$\mathbf{v}_h(t) = \mathbf{v}(t) \cdot \sin(\gamma(t)) \quad (5)$$

The differentiation of equations (3), (4) and (5) results in second order differential equations, which rearranged can be rewritten respectively by (6), (7) and (8):

$$\mathbf{a}_x(t) = \dot{\mathbf{v}}(t) \cdot \cos(\chi(t)) \cdot \cos(\gamma(t)) - \mathbf{v}_y(t) \cdot \dot{\chi}(t) - \mathbf{v}_h(t) \cdot \cos(\chi(t)) \cdot \dot{\gamma}(t) \quad (6)$$

$$\mathbf{a}_y(t) = \dot{\mathbf{v}}(t) \cdot \sin(\chi(t)) \cdot \cos(\gamma(t)) + \mathbf{v}_x(t) \cdot \dot{\chi}(t) - \mathbf{v}_h(t) \cdot \dot{\gamma}(t) \quad (7)$$

$$\mathbf{a}_h(t) = \dot{\mathbf{v}}(t) \cdot \sin(\gamma(t)) + \frac{\mathbf{v}_y(t)}{\sin(\chi(t))} \cdot \dot{\gamma}(t) \quad (8)$$

Knowing that $\dot{\chi}(t)$ is the rate of horizontal angular variation and $\dot{\gamma}(t)$ is the rate of vertical angular variation of the object in spatial displacement.

For the model, the performance of the tangential acceleration \mathbf{a}_{tg} (9) was considered, which is tangential to the movement and causes the variation of the module of the body speed and the centripetal acceleration \mathbf{a}_{cp} , which is perpendicular to the movement and modifies the speed direction, having a horizontal component $\mathbf{a}_{cp\chi}$ (10) and another vertical $\mathbf{a}_{cp\gamma}$ (11).

$$\mathbf{a}_{tg} = \dot{\mathbf{v}}(t) \quad (9)$$

$$\mathbf{a}_{cp\chi} = \dot{\mathbf{v}}(t) \cdot \dot{\chi}(t) = \dot{\mathbf{v}}(t) \cdot \omega_\chi(t) \quad (10)$$

$$\mathbf{a}_{cp\gamma} = \dot{\mathbf{v}}(t) \cdot \dot{\gamma}(t) = \dot{\mathbf{v}}(t) \cdot \omega_\gamma(t) \quad (11)$$

2.1 CV and CT Models

In the CV model, the object moves at a constant speed and in a straight line (Agner Júnior et al., 2020). Thus, $\mathbf{v}_x(t)$, $\mathbf{v}_y(t)$ and $\mathbf{v}_h(t)$ are constant and \mathbf{a}_{tg} , $\mathbf{a}_{cp\chi}$ and $\mathbf{a}_{cp\gamma}$ are null. Consequently, $\mathbf{a}_x(t)$, $\mathbf{a}_y(t)$ and $\mathbf{a}_h(t)$ are null. Thus, the CV and CT model developed in Agner Júnior et al. (2020) was adopted, using the same process equations.

Equation (13), where some of its components remain highlighted due to space limitations, we present the process equation used for the CT model.

$$a_{16} = b_{23} = -\cos(\chi_k) \omega_{\gamma k} \frac{T_k^2}{2}; a_{24} = -\omega_{\chi k} - \cos(\chi_k) \frac{\omega_{\gamma k}^2}{\sin(\chi_k)} \cdot \frac{T_k^2}{2};$$

$$a_{26} = -\cos(\chi_k)\omega_{\gamma k} T_k + \text{sen}(\chi_k)\omega_{\chi k}\omega_{\gamma k}\frac{T_k^2}{2}; a_{36} = b_{43} = -\text{sen}(\chi_k)\omega_{\gamma k}\frac{T_k^2}{2}; a_{44} = 1 - (\omega_{\chi k}^2 + \omega_{\gamma k}^2)\frac{T_k^2}{2}; a_{46} = -\text{sen}(\chi_k)\omega_{\gamma k} T_k - \cos(\chi_k)\omega_{\chi k}\omega_{\gamma k}\frac{T_k^2}{2}; \text{ and } a_{66} = 1 - \omega_{\gamma k}^2\frac{T_k^2}{2}.$$

$$\hat{X}_{k+1|k} = \begin{bmatrix} 1 & T_k & 0 & -\omega_{\chi k}\frac{T_k^2}{2} & 0 & a_{16} & 0 & 0 \\ 0 & 1 - \omega_{\chi k}^2\frac{T_k^2}{2} & 0 & a_{24} & 0 & a_{26} & 0 & 0 \\ 0 & \omega_{\chi k}\frac{T_k^2}{2} & 1 & T_k & 0 & a_{36} & 0 & 0 \\ 0 & \omega_{\chi k}T_k & 0 & a_{44} & 0 & a_{46} & 0 & 0 \\ 0 & 0 & 0 & 0 & \frac{\omega_{\gamma k}}{\text{sen}(\chi_k)}\frac{T_k^2}{2} & 1 & T_k & 0 \\ 0 & \frac{\omega_{\gamma k}\omega_{\chi k}}{\text{sen}(\chi_k)}\frac{T_k^2}{2} & 0 & \frac{\omega_{\gamma k}}{\text{sen}(\chi_k)}T_k & 0 & a_{66} & 0 & 0 \\ 0 & 0 & 0 & 0 & 0 & 0 & 1 & 0 \\ 0 & 0 & 0 & 0 & 0 & 0 & 0 & 1 \end{bmatrix} \cdot \hat{X}_{k|k} \quad (13)$$

$$+ \begin{bmatrix} \frac{T_k^2}{2} & T_k & 0 & \omega_{\chi k}\frac{T_k^2}{2} & 0 & 0 & 0 & 0 \\ 0 & -\omega_{\chi k}\frac{T_k^2}{2} & \frac{T_k^2}{2} & T_k & 0 & \frac{\omega_{\gamma k}}{\text{sen}(\chi_k)}\frac{T_k^2}{2} & 0 & 0 \\ 0 & b_{23} & 0 & b_{43} & \frac{T_k^2}{2} & T_k & 0 & 0 \\ 0 & 0 & 0 & 0 & 0 & 0 & T_k & 0 \\ 0 & 0 & 0 & 0 & 0 & 0 & 0 & T_k \end{bmatrix}^T \cdot [w_x \ w_y \ w_z \ w_\chi \ w_\gamma]^T$$

According to Kang (2008), we can assume the noises w_x , w_y , w_h , w_χ and w_γ as independent with zero mean and variances σ_x^2 , σ_y^2 , σ_h^2 , $\sigma_{\omega_\chi}^2$ and $\sigma_{\omega_\gamma}^2$ respectively. For the covariance matrix of the noise associated with the state (Q_k), we will assume $\sigma_x^2 = \sigma_y^2 = \sigma_h^2 = \sigma_q^2$. Q_k is obtained by doing: $Q_k = E[W_k \cdot W_k^T]$.

2.2 Definition of the Measure Equation

The radar system provides the vector of measurements \mathbf{z}_k in polar coordinates. In order to relate this vector to the vector of states of the target \mathbf{x}_k (defined in Cartesian coordinates), it was necessary to apply a nonlinear transformation, so that \mathbf{z}_k would be written as $\mathbf{z}_k = [\mathbf{x}_k^z \ \mathbf{v}_{\chi k}^z \ \mathbf{y}_k^z \ \mathbf{v}_{\gamma k}^z \ \mathbf{h}_k^z \ \mathbf{v}_{h k}^z \ \omega_{\chi k}^z \ \omega_{\gamma k}^z]^T$, with the measurement having Cartesian coordinates before entering the filter, and then, due to the nonlinear nature of the transformation, there was a need to use the equations of the Extended Kalman Filter, to treat nonlinearity.

Using a trigonometric transformation function, the distance (\mathbf{r}_k), azimuth angle (θ_k) and elevation angle (ϕ_k) measurements, obtained in a polar coordinate system, position components in Cartesian coordinates (x , y and h) as presented in (14):

$$\mathbf{x}_k^z = \mathbf{r}_k \cos(\theta_k) \cos(\phi_k); \ \mathbf{y}_k^z = \mathbf{r}_k \text{sen}(\theta_k) \cos(\phi_k); \ \text{ and } \ \mathbf{h}_k^z = \mathbf{r}_k \text{sen}(\phi_k) \quad (14)$$

2.2.1 Discrete Least Squares Approximations

The data obtained from radar measurements are never accurate, as they may contain inherent errors that, in general, are not predictable, due to the factors already mentioned. Thus, it is unreasonable to require that an approximation function exactly matches the data. According to Burden, Faires and Tasks (2008) such a function would introduce oscillations that were not originally present. The need then arises to determine a function that adapts to a given set of points in a series of inaccurate measurements. According to Burden, Faires and Tasks (2008), the Least Squares Method (LSM), is a way of determining a polynomial approximation function. This method consists of finding the function that best fits the given set of points. The LSM minimizes the error resulting from the adjustment, by adding the squares of the differences between the tabulated values and the values obtained by the approximation. As input data for the LSM, the current position measurement data \mathbf{z}_k , and the two previous positions (\mathbf{z}_{k-1} and \mathbf{z}_{k-2}) were used with the time T_k that these measurements occur.

Thus, we have the problem of approximating each of the three sets of ordered pairs (M_k, T_k) , where $M_k = x_k, y_k$ and z_k ; and $k = 0, 1$ and 2 , by a polynomial of the second degree described by (15):

$$P_M(T) = \sum_{k=0}^2 a_{kM} T^k, \text{ where } M = x, y \text{ and } z \quad (15)$$

One must then find the constants a_{0M}, a_{1M} and a_{2M} that minimize the sum of the squares of the deviations (E):

$$E = \sum_{k=0}^2 (M_k - P(T_k))^2 = \sum_{k=0}^2 (M_k)^2 - 2 \sum_{k=0}^2 P(T_k) \cdot M_k + \sum_{k=0}^2 (P(T_k))^2 \quad (16)$$

$$E = \sum_{k=0}^2 (M_k)^2 - 2 \sum_{k=0}^2 \left(\sum_{j=0}^2 a_j T_k^j \right) \cdot M_k + \sum_{k=0}^2 \left(\sum_{j=0}^2 a_j T_k^j \right)^2 \quad (17)$$

$$E = \sum_{k=0}^2 (M_k)^2 - 2 \sum_{j=0}^2 a_j \cdot \left(\sum_{k=0}^2 M_k T_k^j \right) + \sum_{j=0}^2 \sum_{n=0}^2 a_j a_n \left(\sum_{k=0}^2 T_k^{j+n} \right) \quad (18)$$

For E to have a minimum it is necessary that:

$$\frac{\partial E}{\partial a_j} = 0, j = 0, 1 \text{ and } 2 \quad (19)$$

$$\frac{\partial E}{\partial a_j} = -2 \sum_{k=0}^2 M_k T_k^j + 2 \sum_{n=0}^2 a_n \sum_{k=0}^2 T_k^{j+n} \quad (20)$$

The one described in Equation (19), constitutes a system of $n + 1$ (in this case 3) unknowns a_j and $n + 1$ equations (in this case also 3), called normal equations (21):

$$\sum_{n=0}^2 a_n \sum_{k=0}^2 T_k^{j+n} = \sum_{k=0}^2 M_k T_k^j, j = 0, 1 \text{ and } 2 \quad (21)$$

These last equations (21) can be written as a system in the form:

$$\begin{cases} a_{0M} \sum_{k=0}^2 T_k^0 + a_{1M} \sum_{k=0}^2 T_k^1 + a_{2M} \sum_{k=0}^2 T_k^2 = \sum_{k=0}^2 M_k T_k^0 \\ a_{0M} \sum_{k=0}^2 T_k^1 + a_{1M} \sum_{k=0}^2 T_k^2 + a_{2M} \sum_{k=0}^2 T_k^3 = \sum_{k=0}^2 M_k T_k^1 \\ a_{0M} \sum_{k=0}^2 T_k^2 + a_{1M} \sum_{k=0}^2 T_k^3 + a_{2M} \sum_{k=0}^2 T_k^4 = \sum_{k=0}^2 M_k T_k^2 \end{cases} \quad (22)$$

Thus, solving the system described in (22), for the three values of M , where: M and $M_k = x_k, y_k$ and z_k ; $k = 0, 1$ and 2 , we find the values for the constants a_{0M}, a_{1M} and a_{2M} for the three coordinates (x, y, z) . Thus, substituting in Equation (15) we obtain the three polynomials that roughly describe the position of the target in Cartesian coordinates, as a function of time. With these polynomials, we apply the derivative as a function of time to obtain the polynomial that describes the velocities in Cartesian coordinates:

$$v_M = \frac{d(P_M(T))}{dT}, \text{ where } M = x, y \text{ and } z \quad (23)$$

In this way, we obtain the value of the velocities in x, y and z for the vector of measurements \mathbf{z}_k , replacing the value of T , of the current measure, in the polynomials of (23). The azimuth and elevation angles of the target, in each sampling, are obtained from the projection of these velocity vectors. Thus, the angular velocity $\omega_{\gamma k}^z$ could be obtained from the difference between the current and previous azimuth angle, divided by time. The same procedure was applied to obtain $\omega_{\gamma k}^z$, from the elevation angle. Following the same principle, angular accelerations, which were used in the matrix H_{k+1} , were obtained from the difference between the current and the previous angular velocity, divided by the time between them.

The same procedures used in Agner Júnior et al. (2020) were adopted to perform a nonlinear transformation of the target position and obtain the measurement vector used, given by \mathbf{r}_k, θ_k and ϕ_k .

The covariance matrix of the noise associated with the measure (R_{k+1}), the nonlinear vector function that relates the state variables to the measures, denoted by $fh(k+1, \mathbf{x}_{k+1})$ and the matrix resulting from the Jacobian matrix calculation the function $fh(k+1, \mathbf{x}_{k+1})$ denoted by H_{k+1} , were the same as those used in Agner Júnior et al. (2020).

For initialization of the models, the first two samples were considered, as presented in Agner Júnior et al. (2020). One method of initializing the covariance matrix is to define it as $P_{0|0} = \alpha^2 \cdot Q_k$, the typical value being $\alpha = 10$. Q_k represents the covariance of errors associated with the process.

Process noise was adopted as white when accelerating for the models used. The standard deviation of the process noise (σ_q) for the CV model was defined as in Agner Júnior et al. (2020), $\sigma_q = \alpha \cdot a_{max}$, where $0 < \alpha < 1$ and a_{max} is the maximum acceleration, and were defined empirically as $\alpha = 0.7$ and $a_{max} = 5\text{m/s}^2$, with that, $\sigma_q = 3,5\text{m/s}^2$. In the CT model, the noise level is higher than in the CV model, as the uncertainty is greater at the time of the maneuvers. Empirically defined and $\alpha = 0.8$ and $a_{max} = 125\text{m/s}^2$, the standard deviation of the process noise ($\sigma_q = 100\text{m/s}^2$), the noise in the turning rates as $\sigma_{\omega_x} = \sigma_{\omega_y} = 0,044\text{rad/s}^2$, the noise of angular acceleration rates ($\sigma_{\dot{\omega}_x} = \sigma_{\dot{\omega}_y} = 5\text{rad/s}^2$) for the CT. The measurement noise depends directly on the characteristics of the modeled sensor. In the trajectories in which these noises were considered, a standard deviation was used in the distance of $\sigma_r = 75\text{m}$, in the azimuth angle of $\sigma_\theta = 0,0175^\circ$ and in the elevation angle of $\sigma_\phi = 0,0175^\circ$, as in Agner Júnior et al. (2020) and Frencl (2010).

For the definition of the elements of the transition matrix (Π) of the IMM algorithm, the time interval for obtaining each sample of 4 seconds was adopted, the estimated time for the displacement permanence in a linear manner of 200 seconds (CV) and the estimated time for a 20-second nonlinear trajectory (CT), thus Π is given by (24):

$$\Pi = \begin{bmatrix} 0,99 & 0,01 \\ 0,1 & 0,9 \end{bmatrix} \quad (24)$$

3 Simulation Results

To evaluate the model, a comparison was made with some results presented in Agner Júnior et al. (2020), Frencl (2010) and Frencl and Val (2012b). These were chosen for comparison with the results of this work, as they present three-dimensional models with innovative techniques. In Agner Júnior et al. (2020), a new 3D model was proposed to be applied with KF and EKF, in Frencl (2010) and Frencl and Val (2012b) there was innovation related to the calculation of angular velocity. These studies have tests

described in a level of detail sufficient to allow their reproduction and comparison. The trajectories compared to are zigzag type, formed by seven stretches, as in Figure 1 (a).

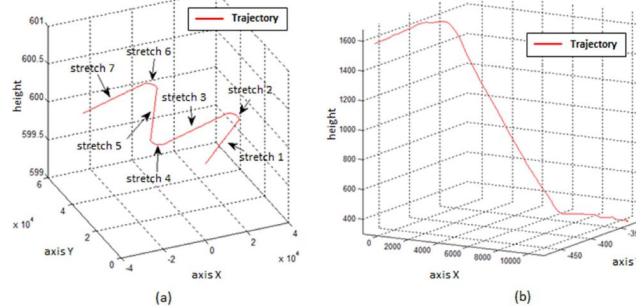


Fig. 1 (a) Zigzag Maneuver Trajectory. (b) Actual trajectory with altitude change.

The measure used to evaluate this work was the RMS error obtained by comparing the trajectory predicted by the model at each instant with the actual future position of the object, for the different displacements performed with time evolution for the position vector, given by (25), where k is the order of counting the samples, i are the Cartesian axes, $res_k^i \in \mathbf{R}$ are the residual vectors calculated by the differences between the position of the sample and the position estimate calculated by the models, and n is the number of data from the trajectory or the stretch of the trajectory. From the n values obtained from RMS_k^i , the average RMS was calculated for each position component, given by (26). The criteria adopted by Agner Júnior et al. (2020) and Frencl (2010), also used here, were the average of RMS_i (32), and the norm of \overline{RMS} (26):

$$RMS_k^i = \sqrt{\frac{1}{k} (res_k^i)^T res_k^i}, k = 1, 2, \dots, n; i = x, y \text{ or } h \quad (25)$$

$$\overline{RMS}_i = \frac{\sum_{k=1}^n RMS_k^i}{n}, k = 1, 2, \dots, n; i = x, y \text{ or } h; \|\overline{RMS}\|_{xyh} = \sqrt{RMS_x^2 + RMS_y^2 + RMS_h^2} \quad (26)$$

In order to make it possible to compare the works, the same adjustment parameters mentioned in Agner Júnior et al. (2020) and Frencl (2010) were adopted. Therefore, $T = 4s, \sigma_r^2 = 75^2, \sigma_\chi^2 = 0,0175^2$ and $\sigma_\gamma^2 = 0,0175^2$, where T is the sampling period, σ_r^2 is the variance of the radar range, σ_χ^2 is the azimuth angle variance and σ_γ^2 is the elevation angle variance. As in Agner Júnior et al. (2020) and Frencl (2010), the initial state estimate was used: $\hat{\mathbf{x}}_{0|0} = [-30000m \ 196,16m/s \ -30000m \ 154,98m/s \ 600m \ 0 \ 0]^T$.

One of the trajectories used for comparison with Agner Júnior et al. (2020) and Frencl (2010) was that of a plane with a vertical inclination of 30° in relation to the horizontal plane xy .

Comparing (a) and (b) of Figure 2, the model of this work performed better than that of Agner Júnior et al. (2020) and Frencl (2010), both for each of the seven stretches presented and for the trajectory as a whole.

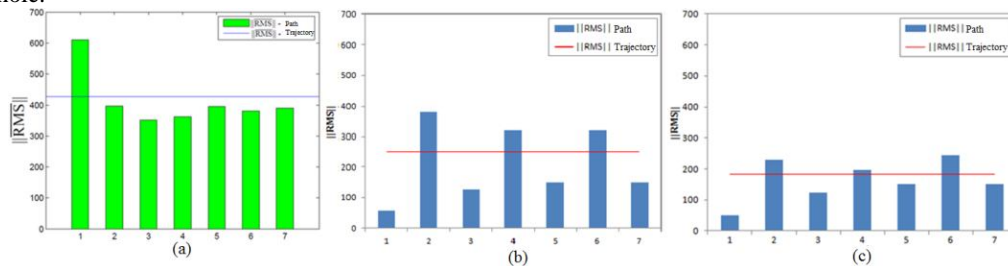


Fig. 2 $\|\overline{RMS}\|$ chart. Plane of 30° . (a)Source:Frencl (2010). (b)Source:Agner Júnior et al. (2020). (c)Result of this work.

The other way used to evaluate the effectiveness of the model described in this study was the comparison with real data. Simulations were carried out to compare the model presented, using the

hypotheses adopted for the noise described above, with the real system used in a Brazilian Navy Ship (BNS). The actual aircraft trajectory data used in the tests were obtained from the Operational Evaluation (OE) tests of a BNS. The OE tests were designed to verify the result of a shooting solution for firing a 4.5-inch cannon projectile, when tracking aircraft. The Cartesian system (x, y, h) was used as the source reference. The trajectories were covered by the aircraft with a speed of around 360km/h. The first two trajectories were traveling a path with upward vertical movement (illustrated in Figure 1 (b)), and the third followed a path with horizontal change of course. The starting and ending positions of the three trajectories were the same as those used by Agner Júnior et al. (2020). For the first trajectory, the comparison between results showed an improvement of 88.995% in the performance of the proposed model when compared to the data obtained in the OE. For the second, it showed an improvement of 87.838% and for the third, an improvement of 72.307%.

4 Conclusion

To handle forecasting the position of objects with a change in their displacement profile. Three-dimensional Constant Speed and Constant Turn models were chosen, which are based on the Cartesian coordinate system. Analyzing the results of the tests performed with these models presented, it is possible to verify that both the CV and the three-dimensional CT, were able to satisfactorily estimate a next position based on the positions of the previous samples for all the tested paths. The CT model is the most significant, as it can work in arbitrary planes of space, increasing the possibility of being able to maintain an adequate prediction of the position of objects during their displacement. The trajectory described by the accompanied object may be contained in a plane parallel to that formed by the x and y axes, but which is rotated on the z axis. The proposed approach was validated by the results of the tests presented, which were compared with the results of other works in the literature and also using real data obtained from BN. Thus, the main contribution of this work was to obtain the scalar velocities of each Cartesian axis to be part of the vector of \mathbf{z}_k . These velocities were deduced from three linear functions, one for each Cartesian axis, obtained from the derivative of three second degree functions elaborated by the Method of Least Squares, from the target position data of the current measure and two previous measures, resulting in greater accuracy than in previous work for tracking maneuver target using 3D position forecast model.

5 References

- Agner Júnior J, Schulze B, Ferro M, Martins ER, dos Santos M (2020). Modelo para previsão de posição de objetos em 3D/3D object position forecast model. *Brazilian Journal of Development*, 6(1), 1873-1890 (2020).
- Frencl VB, Val JB (2012a). Tracking with range rate measurements: Turn rate estimation and particle ltering. In: *IEEE. Radar Conference (RADAR)*, 2012 IEEE. [S.l.], 2012. p. 0287-0292. 2
- Yuan X, Lian F, Han C (2014). Models and algorithms for tracking target with coordinated turn motion. *Mathematical Problems in Engineering*, Hindawi Publishing Corporation, v. 2014. 2
- Liu H, Zhou Z; Yu L; Lu C (2018). Two unbiased converted measurement Kalman filtering algorithms with range rate, *IET Radar, Sonar & Navigation*, 2018, 12, (11), p. 1217-1224, DOI: 10.1049/iet-rsn.2018.5154.
- Bar-Shalom Y, Li XR, Kirubarajan T (2001). Estimation with applications to tracking and navigation: theory algorithms and software. [S.l.]: John Wiley & Sons, 2001. 2, 3, 7, 11
- Korbicz J, et al (2004). Fault diagnosis. Models, artificial intelligence, applications. [S.l.]: Springer Berlin/Heidelberg, 2004.
- Bar-Shalom Y, et al (1988). Mathematics in science and engineering. [S.l.]: Academic press, 1988. 3
- Frencl VB (2010). Técnicas de filtragem utilizando processos com saltos markovianos aplicados ao rastreamento de alvos móveis. *Dissertação (Mestrado) - Universidade Estadual de Campinas (UNICAMP)*, 2010. 3, 12, 13
- Welch G, Bishop G (2001). Course 8-an introduction to the kalman filter. *SIGGRAPH 2001 Courses*, 2001. 3
- Kang E (2008). Radar System Analysis, Design, and Simulation. [S.l.]: Artech House, 2008. ISBN 9781596933477. 8
- Burden RL, Faires JD, Tasks A (2008). Análise numérica. [S.l.]: Cengage Learning, 2008. 8, 9
- Frencl VB, Val JB (2012b). Rastreamento utilizando Filtro de Partículas com Perturbação Gaussiana na Estimativa e Medidas de Velocidade Radial, 09/2012, XIX Congresso Brasileiro de Automática, Vol. CD, pp.4435-4442, Brasil, 2012.